February 2007

B_c studies at ATLAS

Master of Science Thesis
by

Caroline Laaksometsä

DEPARTMENT OF PHYSICS, LUND UNIVERSITY

Abstract

This thesis investigates the possibility of studying the strong force by studying the B_c meson at ATLAS.

The strong force acting between quarks grows with distance and this is one of the complications that contribute to why there is no unique theory describing the force at all energies. This in turn means that the potential created by the force cannot be derived from first principles. To get a better picture of this potential a system that enables comparison between a theoretical model and experiment is needed, a system fulfilling this requirement is the B_c meson. The potential created between the $\bar{b}$- and c-quark is “easily” predicted by models due to that it behaves non-relativistically and it gives a clear experimental signal which makes it easy to treat experimentally.

Before the actual search for different mass states of the B_c meson can be started, the signal and background has to be throughly investigated with simulations to make certain that all cuts in the off-line analysis are optimized.

Contents

1 Introduction

Physicists seek a way to describe the behavior of bodies. Everything from falling bodies to confined quarks is described with mathematics and theoretical models. The theories are tested by experiments to be disregarded or accepted. In particle physics experiments it is not always the particle that is detected. Sometimes the particles are too unstable to reach the detector and then the decay products are detected instead. These signals are then studied and compared to what the model predicts. The answers in particle physics are not always unambiguous after experiments have been performed because it is possible that several models with completely different physical assumptions can predict the same outcome. For example, the banana peel in the cartoon in Fig. 1.1 can come from a baboon as well as a chimpanzee.

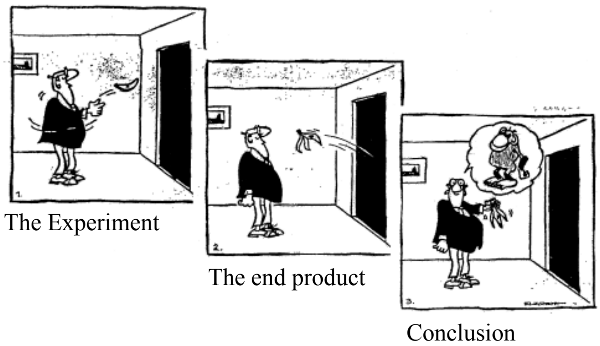

Fig. 1.1 Experimental investigation.

To get a better answer to the question who ate the banana there is a need for further experiments and maybe even a need doing studies on peeling patterns for baboons and chimpanzees. This uncertainty and the need for thinking of every possibility make experimental particle physics both challenging and interesting.

1.1 The standard model

The particle physicists' goal is to find the smallest particles that build up our world and to understand their behaviour. The theoretical model that is nearest this goal is called the standard model. It states that elementary particles can be divided into two categories; spin one-half particles called fermions and particles with integer spin called bosons. Fermions build up matter and the forces between these are mediated by bosons. The fermions are divided into two groups; quarks and leptons. Leptons are freely existing particles whiles quarks are the elementary particles building up other particles. All non-elementary particles consist of a combination of two or three quarks, called mesons and baryons respectively.

There are four forces and all of them are intermediated by bosons. The graviton (not yet experimentally found) intermediates the gravitational force that is for example, responsible for us staying on the Earth's surface. The weak force is intermediated by weak bosons. It can change the flavour of a quark, and an electron, for example, can transfer into an electron-type neutrino by emitting a W boson. The electromagnetic force acting between charged particles is carried by the photon. The strong force, which is intermediated by gluons, is responsible for holding quarks together in hadrons. All the elementary particles known today and the three forces for which intermediating particles have been found are summarized in Table 1.1.

		Generation	*1st*	*2nd*	*3rd*
Fermions	Quarks		$\begin{pmatrix} u \\ d \end{pmatrix}$	$\begin{pmatrix} c \\ s \end{pmatrix}$	$\begin{pmatrix} t \\ b \end{pmatrix}$
	Leptons		$\begin{pmatrix} e \\ \nu_e \end{pmatrix}$	$\begin{pmatrix} \mu \\ \nu_\mu \end{pmatrix}$	$\begin{pmatrix} \tau \\ \nu_\tau \end{pmatrix}$

Bosons

Interaction	**Particle**	**Mass (GeV)**
Electromagnetic	γ (photon)	0
Weak	$W^{\pm}$, Z^{o} (weak bosons)	80.22,91.19
Strong	g (gluon)	0

Table 1.1 The elementary particles and forces of the standard model.

This thesis is mainly going to discuss the B_c meson, a meson consisting of one c -quark and one $\bar{b}$ -quark, and the strong force.

1.2 The strong force

The part of the standard model that describes the strong interaction is called the Quantum Chromodynamics, QCD. The part Chromo in the name refers to the fact that gluons couple to a property called colour. Colour in QCD is analogous to charge in Quantum Electrodynamics, QED. The differences are that the gluons carry colour while the photons are electrically neutral, and that there exist three colours, red, green and blue, and the associated anticolours anti-red, anti-blue and anti-green compared to the one electric charge in QED. The strong force is flavour independent and consequently it acts in the same way for all six quarks.

Another property of the strong force is that it grows as the distance between the partons grows, in opposite to the electromagnetic force that decreases with distance. At very short distances quarks and gluons are almost free particles. This somewhat surprising behavior of the strong force is called asymptotic freedom. The asymptotic freedom in turn leads to another property of the strong force called colour confinement, which states that no coloured particles can exist isolated. If two quarks are separated the force between them grows until the energy is big enough for new quarks to be created and forming new colourless hadrons. The colour confinement has its origin in the self-coupling of the gluons which is possible since they carry colour. This is the reason why single quarks never have been observed. The strength of the strong force is given by the strong coupling constant, α_s and as mentioned it decreases with energy, as shown in Fig 1.2.

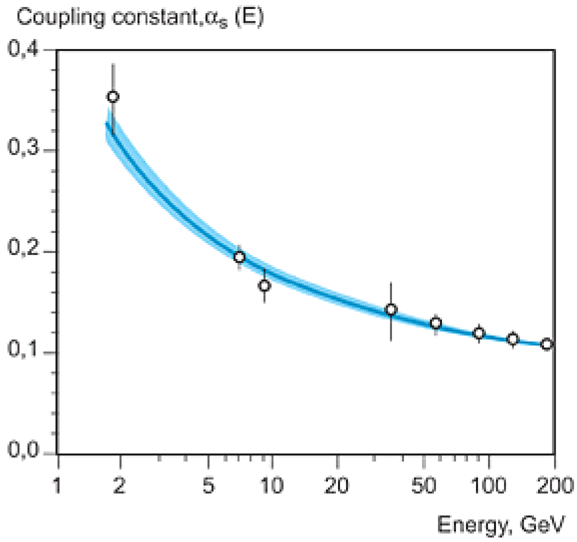

Fig. 1.2 The strong coupling constant α_s as a function of the energy. The curve has a negative derivate or negative beta-function that it is also called. [1]

The strong coupling constant is called a running constant since it varies over energy, so when dealing with this force it is important to state which energy scale is utilized so that the appropriate value of the constant is used. At large energies the strong force can be treated in the same way as the electromagnetic force, which can be described by using perturbation calculations. The pertubative treatment is possible since the electromagnetic coupling constant is small compared to 1 and so is the strong coupling constant at large energies. This leads to that the strong force equations can be expanded as a series according to the order of the strong coupling constant, i.e. the high orders in α_s can be treated as a pertubation. Nonetheless there is no field theory describing the strong force at all energies.

1.2.1 Spectrum of the strong force

The strong force creates a potential that confines the quarks. This potential together with the wave-function of the quark system gives the mass spectrum of the particle.A diagram of the energies at which the particle has bound states is called the spectrum. There exist several theoretical models that predict the shape of this potential. The bound states that the potential gives are experimentally searched for in order to verify or reject the prediction. Most models include a Coulomb term ~1/r, and a confinement term which is linear ~r according to Eq. 1.1 [2].

$$V_{conf}(r) = -\frac{4\alpha_s}{3r} + br \qquad (1.1)$$

where b is a free parameter and r is the distance between the quarks.

The Coulomb term appears always when there is an exchange of massless particles, in this case the gluons. This term grows for small r and is therefore most important at small distances. On the contrary the linear term determines the behaviour of the quarks at large distances. The theoretical models usually also include a spin dependent part arising from the interaction of the spins of the quarks, Eq. 1.2:

$$V(r) = V_{gconf} + V_{spin} \qquad (1.2)$$

The spin part of the potential is responsible for the fine splitting of the potential levels.

1.3 The ATLAS experiment

Atlas, **A T**oroidal **L**HC **A**pparatu**S,** is one of the four experiments at LHC (Large Hadron Collider) constructed at CERN. LHC is a ring with a circumference of 27 km, it is located 100 m underground just outside Geneva in Switzerland. The LHC will be commissioned in the summer of 2007. In the LHC ring protons are accelerated in both directions. The acceleration is accomplished by strong electric fields and the particle beams are bent by superconducting magnets producing a magnetic field of 8 Tesla. The protons are gathered in bunches, there are 2835 bunches separated by 7.5 m (25 ns) and each bunch contain 10^{14} protons. The protons will collide at four points around the ring, at these points detectors are constructed to register the end products of the collisions. The energy at the collisions will be the highest energy produced in a particle accelerator ever, namely 14 TeV[1]. New physics is expected to be found in this new energy scale, and the high luminosity at LHC will increase the probability of finding new physics. Luminosity is a measure of number of particles per square centimeter and second in the beam.

The ATLAS detector is not designed to detect a particular physical process. Instead it is able to measure a variety of different particles with a broad energy range, it is a general-purpose detector.

1.3.1 ATLAS coordinate system

The ATLAS coordinate system is a right-handed system, in which the positive x-axis points towards the center of the accelerator ring, the y-axis upwards and the z-axis follows the ring. The transverse momentum is measured since it is this part of the momentum that is bent in the solenoidal magnetic field. The transverse momentum (p_T) is the component

*1. The unit electron volt (eV) is the kinetic energy an electron gains when it passes an electric potential of 1 volt. 1 eV, that corresponds to 1.602 176 53 * 10^{-19} J, is small energy in particle physics and thus this unit is used with prefixes like Mega (10^6), Giga (10^9) and Tera (10^{12}).*

of the momentum that is in the plane at a right angle to the beam axis, the xy-pane, which is also called the transverse plane. The transverse momentum is obtained by measuring the strength of the magnetic field (B) and the radius (R) of the trajectory produced by the charged particle, these numbers are then put in Eq.1.3 [3] that returns the transverse momentum of that particle.

$$p_T = 0.3ZBR \qquad (1.3)$$

where Z is the charge of the particle in units of e (electron charge), B is in Tesla and R is in meters.

The angle between p_T and the x-axis is called the azimuthal angle and it is denoted by φ. It gives the direction of p_T in the transverse plane. The azimuthal angle is 0 when p_T is pointing into the positive x direction and it grows when going towards the positive y-axis. The angle φ is defined as being in the range [0,2π]. An overview of the angle and momentum definitions is shown in Fig. 1.3.

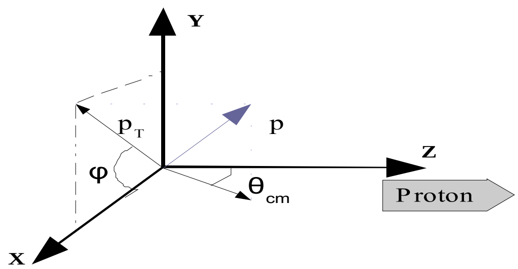

Fig. 1.3 The azimuthal angle and the polar angle.

The angle that gives the direction with respect to the beam axis is called the polar angle, denoted by θ. It is zero when pointing in the positive z direction and it grows when going towards the transverse plane. The angle θ is defined as being in the range [0, π]. The polar angle is most often rewritten in a form called pseudorapidity, denoted by η and defined as in Eq. 1.4 [4]:

$$\eta = -\ln(\tan(\theta/2)) \qquad (1.4)$$

It can be seen as a measure of the closeness to the beam. The pseudorapidity varies from $+\infty$ to $-\infty$ corresponding to θ = 0 and θ = π respectively.

In the ATLAS detector [5] the trajectories of charged particles in the solenoidal field of the inner detector can be described by five helix parameters, see Table 1.2.

Helix parameter	Definition
$1/p_T$	The inverse of the transverse momentum.
Φ	Azimuthal angle.
d_0	Transverse impact parameter, defined as the transverse distance to the track from the beam axis.
$\cot\theta$	Cotangent of the polar angle
z_0	Longitudinal impact parameter, defined as the distance to the track from the beam axis in z-plane.

Table 1.2 Helix parameters used at ATLAS.

1.3.2 The ATLAS detector

The ATLAS detector measures trajectories of charged particles and particle energies. The ATLAS detector system can be divided into four major parts: the inner tracker (IT), the calorimeter (CM), the muon spectrometer (Mu) and the magnetic system (MS), Fig 1.4.

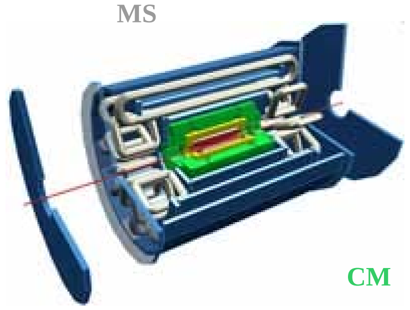

Fig. 1.4 The ATLAS detector.

Allthough $b\bar{b}$ -pairs are produced relatively frequently (once in every 100 collisions), the event selectivity has to be very good, since it is not posible to store all the events on tape or disk. Vertex localization and muon identification are essential ingredients for B-event selection in ATLAS. This is why the inner detector and the muon system are the most important detector elements, and they are briefly introduced here.

The inner detector is a cylinder which is 7 m in length and 1.2 m in radius. It is located inside the central solenoid providing a magnetic field of 2 T. The main purpose of this part is measurements of both momenta and vertices. It is composed of three components: the pixel detectors in the innermost part, as close as 5 cm from the beam, the Semi-Conductor Tracker (SCT) in the middle and the Transition Radiation Tracker (TRT) in the outermost part. All three components have the assignment to measure track hits and since they are inside the central solenoid the tracks will be bent and the transverse momentum can be measured from these hits (see Eq. 1.3). The inner detector has a pseudorapidity coverage of $|\eta|<2.5$.

The muons are heavy enough to pass right through the inner detector and the calorimeters and they are long-lived enough to escape the detector before decaying. Because of these properties the muons must be detected by special systems, called muon spectrometers that identify and measure the momentum. The detectors used for these measurements are monitored drift tube chambers around the beam axis and cathode strip chambers in the forward regions. The drift times for both of these detector types are much larger that the bunch crossing time, but the trigger chambers give the correct timing and reduces the number of events. Resistive plate chambers (RPC) are used in the barrel region and thin gap chambers in the end-cap region. The muon system is embeded in a toroidal magnetic field, created by three huge superconducting toroid magnets (one for the barrel and one for each end-cap).

1.3.3 B-trigger at ATLAS

The LHC bunch crossing rate is 40 MHz. When LHC reaches its design luminosity, $10^{34}cm^{-2}s^{-1}$, the interaction-rate will be 1 GHz. Even at the lower luminosity of $10^{33}cm^{-2}s^{-1}$ the interaction rate is still 100 MHz. This leads to a big amount of data to handle, so big that today's technology is not sufficient. The size of one event is typically 2 MB, so an event rate of 100 MHz would mean an output rate of 200 TB/s. Therefore trigger systems are needed, these have the assignment to select interesting data and stop the uninteresting ones with a good efficiency.

The ATLAS B-physics trigger [6] consists of three levels:

<u>Level 1:</u> Here a low-p_T trigger is used, it selects events which have a muon with p_T>6 GeV. The barrel algorithm takes hits in the inner RPC station and opens a window in the next station. The desired p_T threshold determines the size of this window. For an event to be accepted three out of four layers (there are 2 per station) have to contain hits in the opened window in both (r, η) and (r, φ) projections. The LVL1 accept rate is 75kHz.

<u>Level 2:</u> There are four steps in the Level 2 trigger. In the first step the LVL1 muons are confirmed in the muon spectrometer and inner detector. The LVL2 trigger has a better resolution leading to that muons with p_T below the threshold are rejected. The fraction of muons originating from decays in flight of $\pi^{\pm}$ and $K^{\pm}$ are also reduced due to the matching of track elements between the muon spectrometer and the inner detector. The second step makes a full track search in the TRT and then extrapolates through the rest of the inner detector. When this extrapolation has been done, three-dimensional track reconstruction is possible and this makes the background reduction even better. In the third step the track candidates are extrapolated into the muon spectrometer and the calorimeters that makes the muon/electron identification possible. Finally in the fourth step all the information from previous steps are combined and tested against a list of partial final state hypotheses. The LVL2 accepts events with a 1kHz rate.

<u>Event Filter:</u> The EF uses algorithms similar to the offline reconstruction. For example, impact parameter cuts and vertex reconstruction are used. The EF output rate is about 100Hz.

B physic studies at ATLAS are going to be done in the initial period, when the luminosity is still low, of the order $2*10^{33}cm^{-2}s^{-1}$ or lower. When the accelerator reaches its designed luminosity the amount of data produced is too big for the B-trigger to handle.

The trigger given above is the initial plan. The trigger plans have been updated to lower the number of selected events even further. The main changes concern the LVL1, which now foresees a dimuon trigger instead of a single-muon trigger, and the LVL2, which will use a track search in restricted regions of the TRT instead of searching for tracks in the whole detector volume.

1.4 Experimental signal

For analysis of B-hadron final states in ATLAS, mostly charged particles are used, since the resolution is better for charged than neutral particles in B-decays. To select the signal created by the particle of interest in the offline, analysis selections are applied, for example mass-, charge- and momentum cuts. The values of cuts depend on the particle and the background. The data sample has contributions from signal and background, so the cuts have to set so that background events are not selected. At the same time it is important that a sufficient amount of correctly identified events are selected so that there is enough statistics to make conclusions at the end. In Fig. 1.5 the mass distribution from simulated data from ATALAS is shown with dots and the statical errors are indicated with bars, and a fit to the data is illustrated with a solid curve. The fit is done inside the ROOT program [7] and is usually a Gaussian since N statistically independent measurements approach a Gaussian distribution when N goes to infinity. The three numbers in the upper right corner are the results of the gaussian fit, giving the mean value, the standard deviation and χ^2 of the gaussian. The standard deviation can be interpreted as the measurement resolution. The natural broadness of the mass peak, the width Γ, is defined as in Eq. 1.5:

$$\Gamma=1/\tau \qquad (1.5)$$

where τ is the lifetime. This equation says that if a particle has a small lifetime the peak will be broad. If instead the lifetime is long a narrow peak it observed. For example the B_c meson has the lifetime 0.46 ps and this corresponds to the width $1.43*10^{-4}$ eV. Comparing this to the experimental resolution, which is 60 MeV, it is evident that the B_c signal width originates completely from the experimental resolution.

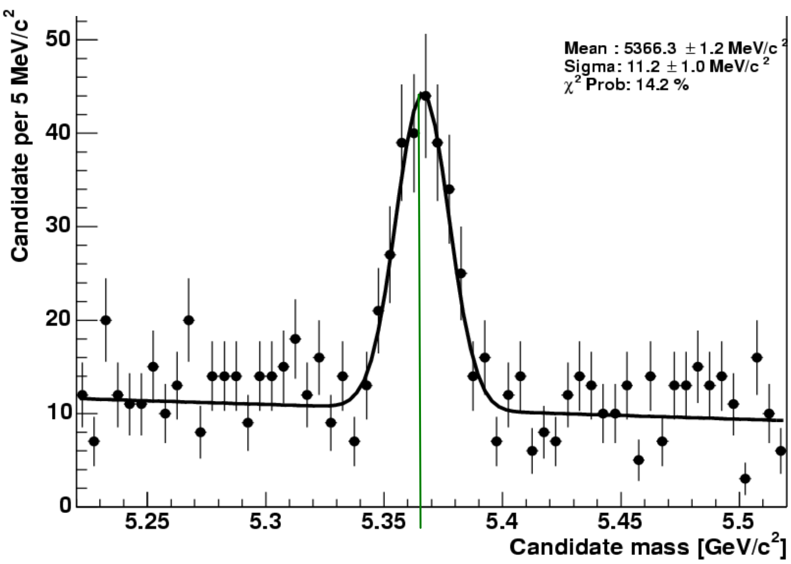

Fig. 1.5 Mass distribution of B_s reconstructed from the decays $B_s \to J/\Psi\ \Phi$.

χ^2 over number of degrees of freedom (χ^2 /NoF) is another number usually given as well. It is a measure of how good a fit is compared to the data or with other words it is a measure of the deviation between the fit and data. The number χ^2 is obtained by comparing the difference between the measured and expected values with the standard deviation, Eq. 1.6. This means that if the difference is small compared to the standard deviation we get a low value of χ^2.

$$\chi^2 = \sum_{i=1}^{k} \frac{(x_i - \mu_i)^2}{\sigma_i^2} \qquad (1.6)$$

where x_i is the measured value for measurement i, μ_i is the expected value and k is the number of degrees of freedoms and σ is the standard deviation. If χ^2 /NoF is much lower or higher then 1 than the fit is not in good agreement with data. The fit can still agree with the data in specific regions but somewhere it fails to predict the data, see Figs. 1.6 and 1.7.

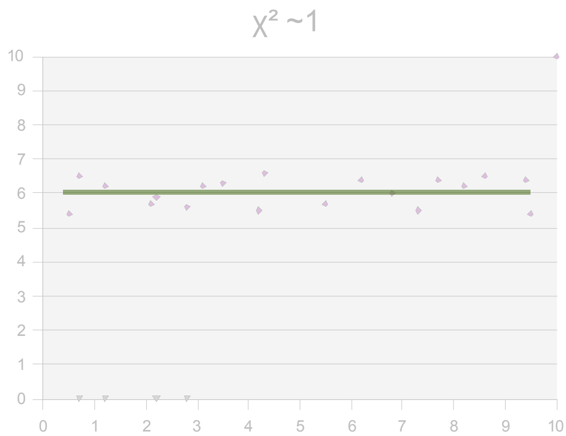

Fig. 1.6 Example of a fit (green line) with χ^2 /NoF close to one.

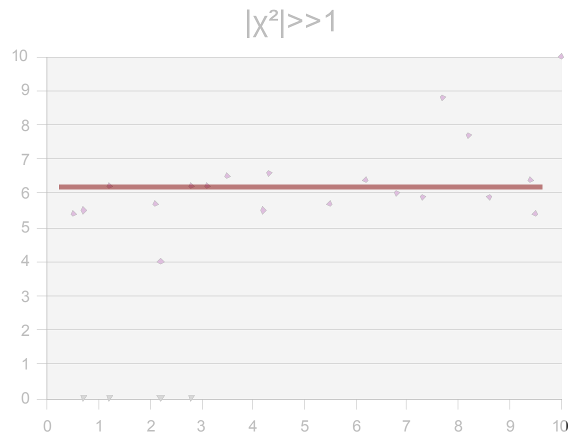

Fig. 1.7 Example of a fit (red line) with χ^2 /NoF not close to one.

1.5 The B_c meson

In order to investigate the shape of the strong force potential, a system that enables comparison between theory and experimental data is needed. That is a particle that gives a spectrum easy to predict theoretically and do measurements on is needed. It is easiest to make predictions on systems consisting of as few bodies as possible. The particles containing the fewest quarks are the mesons. By suppressing the relativistic effect the system becomes even easier to treat. This means that we are interested in mesons built up of the heavy quarks charm and bottom. The top quark is not of interest since it decays before it binds to other quarks and builds a meson. To make the particle easy to find experimentally it must give a clear signal, a peak with small width, if the peak is broad it will dissolve in background. A small width is the same thing as a long lifetime, so the particle has to decay weakly (lifetime=10^{-12}s) and not strongly (lifetime=10^{-20}s). Both bottonium $b\bar{b}$ and charmonium $c\bar{c}$ decay via annihilation by strong force. They have electro-weak decay channels as well, but since the strong decay has a smaller lifetime it is more probable that it decay strongly, and the interesting electroweak decays are rare. The mesons built of one $\bar{b}$ - and one c-quark, called the B_c meson, decay only through electroweak interactions.

Conclusion: The particle of interest to investigate the strong force potential is the B_c meson!

1.5.1 History of the B_c meson.

All ground states of mesons composed of quarks with different flavours, except for the B_c meson, were experimentally found before 1997. There existed several models that predicted the mass and lifetime of the B_c meson, for example some models said that the lifetime should be between 0.4-0.9 ps [8] while others claimed that it should be in the range 1.1-1.4 ps [8]. The large difference in the predictions depends on which of the decay contributions is seen as the largest. There are three major contributions for the decay of B_c and these are:

1. $\bar{b} \rightarrow \bar{c}W^+$ with c as a spectator giving final states $(J/\psi\pi)$ and $(J/\psi l\upsilon)$.
2. $c \rightarrow sW^+$ with b as a spectator giving final states $(B_s\pi)$ and $(B_s l\upsilon)$.
3. $\bar{b}c \rightarrow W$ giving final state $(\tau\nu_\tau)$

In Fig. 1.8 the decays are shown with diagrams.

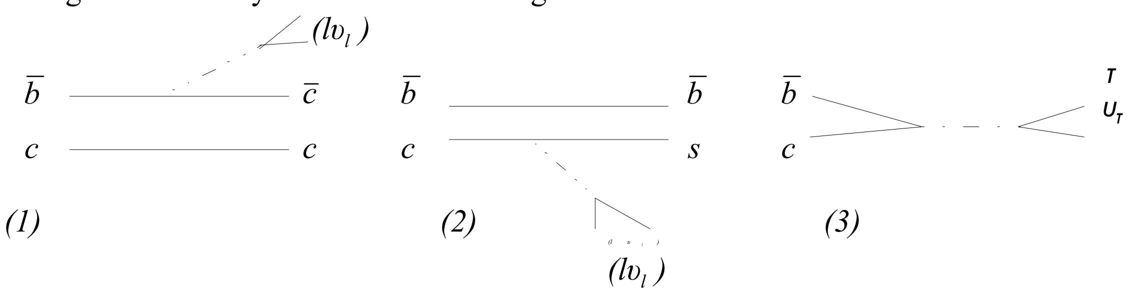

Fig 1.8 Three major parts of the B_c decay.

If no interference is assumed the total decay width can be seen as a sum of the three components, Eq 1.7.

$$\Gamma(B_c \rightarrow X) = \Gamma(b \rightarrow X) + \Gamma(c \rightarrow X) + \Gamma(Anni.) \quad (1.7)$$

Using the spectator approximation, where the effect of the second quark is neglected [9, 10], it is obtained that the three components give the following contributions:

$$\Gamma(b \rightarrow X) = \frac{9G_F^2 |V_{cb}|^2 m_b^5}{192\pi^3} = 8.75 \cdot 10^{-4} eV \tag{1.8}$$

$$\Gamma(c \rightarrow X) = \frac{5G_F^2 |V_{cs}|^2 m_b^5}{192\pi^3} = 4.19 \cdot 10^{-4} eV \tag{1.9}$$

$$\Gamma(Anni.) = \frac{G_F^2 |V_{cb}|^2 f_{B_c}^2 M_{B_c}}{8\pi} \sum m_i^2 \left(1 - \frac{m_i^2}{M_{B_c}^2}\right)^2 C_i = 0.923 \cdot 10^{-4} eV \tag{1.10}$$

where G_F is the Fermi constant, V_{cb} and V_{cs} are CKM matrix elements, m_i is the mass of the heaviest fermion, C_i is a constant which is 1 for the $\tau\nu_\tau$ channel and $3|V_{cs}|$ for $\bar{s}c$. This yields the total width of $13.86*10^{-4}$ eV and a lifetime of about 0.47 ps for the B_c meson.

1.5.2 Measurements

At **CERN** the search for the B_c meson was done at the Aleph, Delphi and Opal experiments. All three studied the decay of the neutral Z boson. There are several alternatives to how the B_c meson can be produced through the decay $Z^0 \to b\bar{b}$:

- A $c\bar{c}$ pair is created from vacuum and then combines with the $\bar{b}$ - and b-quark respectively. This process is suppressed since the creation of a $u\bar{u}$ -pair is 10^{10}-10^{11} times more likely
- The $\bar{b}(b)$ quark emits a virtual W boson and transfer into a $\bar{c}(c)$ quark. This is suppressed by the small CKM element V_{bc} ~0.04.
- The process of a b quarks emitting a hard gluon which fragments to a $\bar{c}c$-pair is of the order α_s^2~ 0.09 and is the dominating process.

Despite that the third process is the dominating one it has a small strength. This is compensated by the big amount neutral Z bosons created at CERN during the run of the LEP accelerator, 1989-2000.

At *Aleph* they search for the decays with final states ($J/\Psi\pi$) and (J l υ_l) in a sample of 3.9 $*10^6$ Z^0 decays and found 2 candidates for the second final state [11]. At *Delphi* they search for decays $B_c \rightarrow$ ($J/\Psi\pi^+$), ($J/\Psi l \nu_l$) and ($J/\Psi\pi^+\pi^-\pi^-$) in a sample of 3.02 $*10^6$ Z^0 decays and they found 1 candidate for each of them. When the mass calculations were done it was evident that one of the cases could not be a B_c meson since the masses found did not agree with each other [12]. At *Opal* they search for decays $B_c \rightarrow$ ($J/\Psi\pi^+$), (J a_l^+) and (J/Ψ l υ_l) and they found 2, 0 and 1 candidates respectively when they looked at 4.02 $*10^6$ Z^0 decays [13].

None of these experiments gave enough information to claim the existence of the B_c meson, instead it was discovered 1998 at **Fermilab** [8]. They searched for the meson in the decay $B_c \rightarrow (J/\Psi$ l $\upsilon_l)$ where charmonium decays into a muon pair. This decay does not have a large branching ratio but the signal is clear and relatively easy to find. The lowest prediction for the lifetime of the B_c meson was sufficiently big so that one expected that the distance between the primary (where the B_c meson was created) and the secondary vertex (where the B_c decayed) was measurable. Thus the signature that they looked for was two coinciding muons with an invariant mass compatible with the mass of charmonium. Charmonium has a short lifetime, as mentioned earlier, meaning that the distance it travels before it decays is negligible and thus the muons can be seen as coming from the secondary vertex as well. In addition to the two muons one lepton passing the same displaced (second) vertex is needed. A fit to experimental results yielded that $20^{+6.2}_{-5.5}$ events originated from the B_c meson and the null hypothesis was rejected at a level of 4.8 standard deviations. The mass and lifetime measured were:

$$m(B_c) = (6.04 \pm 0.39(stat) \pm 0.13(syst))\ \ GeV$$
$$\tau(B_c) = (0.46^{+0.18}_{-0.16}(stat) \pm 0.03(syst))\ \ ps$$

More updated numbers from further measurements are:

$$m(B_c) = (6.286 \pm 0.005(stat) \pm 0.0012(syst))\ \ GeV \qquad [14]$$
$$\tau(B_c) = (0.463^{+0.073}_{-0.065}(stat) \pm 0.036(syst))\ \ ps \qquad [15]$$

1.5.3 Mass spectrum of the ($\bar{b}c$) system

There exist still today several models that predict the spectrum of the B_c meson, most of them gives similar results. The main ideas of and the spectrum given by two of these models are going to be included here, further descriptions of the models can be found in the references.

The two models, both spin-independent, are:

* Buchmüller-Tye potential [16]: They use a flavour independent potential that has emerged from the coinciding experimental data of the two quarkonium potentials in the region 0.1 fm<r<1 fm. It also takes into account the two-loop diagrams appearing at short distances where the energy uncertainty is big enough for them to be created.
* Martin potential [17]: A power potential that relatively accurately predicts the levels of both the bottonium and the charmonium system.

Both potentials give a B_c spectrum looking a lot like the ones for $(\bar{b}b)$ and $(\bar{c}c)$, the difference lies in the jj coupling of the B_c quarks instead of LS coupling as it is for the quarkonium systems. For example the term 1^1S_1 which appears in the B_c spectrum is not possible in LS coupling, |L-S|<J<|L+S|, S=0 and L=0 can never result in J=1! When adding the spin-dependent part as a perturbation the spectrum in Fig. 1.9 is obtained [18]. The levels from the two models are very close to each other and therefore the same spectrum represents both of them. The exact level-values are given in the Table 1.3.

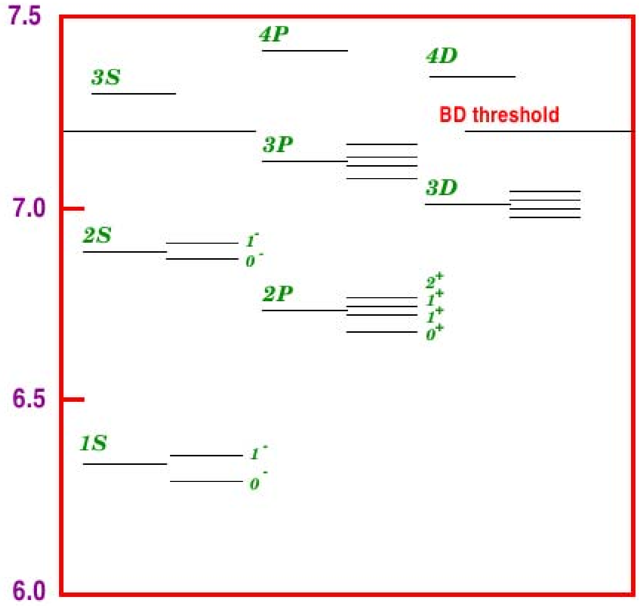

Fig 1.9 The B_c spectrum obtained from BT and Martin potentials with the spin splitting included.

state	Martin	BT
1^1S_0	6.253	6.264
1^1S_1	6.317	6.337
2^1S_0	6.867	6.856
2^1S_1	6.902	6.899
2^1P_0	6.683	6.700
$2P\ 1^+$	6.717	6.730
$2P\ 1'^+$	6.729	6.736
2^3P_2	6.743	6.747
3^1P_0	7.088	7.108
$3P\ 1^+$	7.113	7.135
$3P\ 1'^+$	7.124	7.142
3^3P_2	7.134	7.153
$3D\ 2^-$	7.001	7.009
3^5D_3	7.007	7.005
3^3D_1	7.008	7.012
$3D\ 2'^-$	7.016	7.012

Table 1.3 The exact values predicted by the models .

1.5.4 Production of the B_c meson

The dominant process that produces B_c mesons at large transverse momentum, $p_T >> m(B_c)$, is the fragmentation of a $\bar{b}$ quark. If p_T is small then the recombination of the $(\bar{b}b)$-pair is considerably large and consequently suppressing the production of a B_c meson. The cross section for direct production of a B_c meson at large transverse momentum, Fig. 1.10, can be written as in Eq. 1.11 [19, 20]:

$$d\sigma(B_c(p)) = \int dz d\sigma\left(\bar{b}\left(p/z,\mu\right)\right) D_{\bar{b}\to B_c}\left(z,\mu\right) \qquad (1.11)$$

where z is the energy fraction carried by the B_c meson, μ is the factorization scale and D is the fragmentation function.

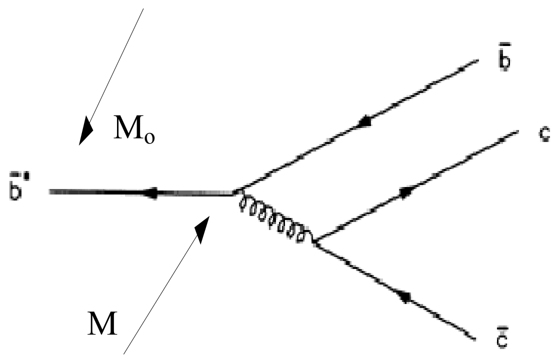

Fig. 1.10 Feynman diagram of the $\bar{b}$ fragmentation into a B_c meson.

The fragmentation function, Eq. 1.12, describes the probability of a parton splitting into a hadron and other partons [21]:

$$D_{\bar{b}\to B_c} = \frac{1}{16\pi^2}\int ds\cdot\theta\left(s-\frac{(m_b+m_c)^2}{z}-\frac{m_c^2}{1-z}\right)\lim\frac{|M|^2}{|M_0|^2} \qquad (1.12)$$

M is the matrix element for the production of a B_c and $\bar{c}$ with total four-momentum q and invariant mass $s=q^2$. M_o is the matrix element for the production of a $\bar{b}$ with the same three-momentum q. These matrix elements can be calculated (done in Ref [21]) and when inserting the results in the equation we get Eq. 1.13 that is the final form of the fragmentation function.

$$D_{\bar{b}\to B_c}(z,m_b+2\mathrm{m}_c) = \frac{2\alpha_s(2\mathrm{m}_c)^2|R(0)|^2}{81\pi\cdot m_c^3}\frac{rx(1-z)^2}{(1-(1-r)z)^6} \qquad (1.13)$$
$$\times(6-18(1-2\mathrm{r})z+(21-74r+68r^2)z^2-2(1-r)(6-9\mathrm{r}+18)z^3+3(1-r)^2)(1-2\mathrm{r}+2\mathrm{r}^2)z^4$$

where R(0) is the non-relativistic radial wave function at the origin for the B_c meson, $r = m_c/(m_b+m_c)$ and μ is set to 2 m_c +m_b, which is the minimum value of the invariant mass for the fragmenting $\bar{b}$ to be able to create the final state B_c. To get the total cross-section for the B_c production the production of excited states of the B_c mesons, B_c^*, have to be taken into consideration. These will cascade to the ground state and thus increase the cross-section. All excited states below 7.15 GeV, which is the BD meson production threshold, have to be considered. The fragmentation function can be calculated for the excited states as well, it will look somewhat different due to the fact that the wave function differs from the ground state wave function. We can see in Fig 1.11 that the fragmentation into B_c or B_c^* has a peak at z~0.9 this means that the B_c/B_c^* meson will have almost the same longitudinal momentum as the $\bar{b}$ quark it hadronized from.

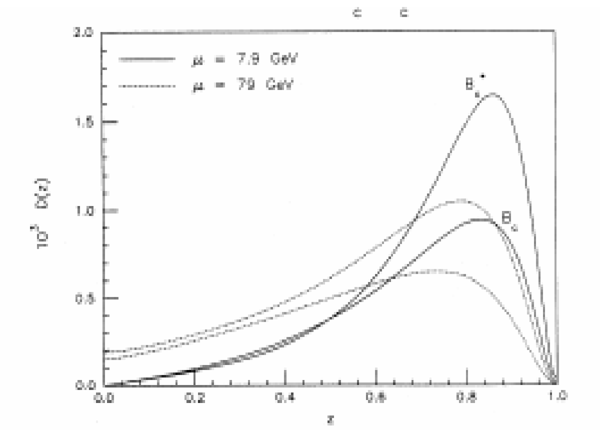

Fig. 1.11 The fragmentation function as a function of z.
Dotted line μ=79 Gev and solid line μ=7.9 GeV.

Another thing that is clear is that the hadronization is bigger for 7.9 GeV than for 79 GeV. The energy 7.9 GeV corresponds approximately to $2m_c+m_b$ and as mentioned above this is the energy needed for creating B_c/B_c^*. If the energy gets much larger, for example 79 GeV, other particles are also produced and this lowers the B_c/B_c^* hadronization. One last thing we can note in the diagram above is that the hadronization into excited states is more probable and this is due to the fact that there are several excited states but just one ground state.

1.5.5 Production of the B_c meson at LHC

At LHC energies the condition of the large transverse momentum is not fulfilled. The transverse momentum available in an accelerator depends on the collision energy. When the energy is big enough the p_T distribution will become more flat, at ”lower” energies the distribution will have a peak at low p_T. At LHC energies the p_T will still have its peak in the lower region. One other feature with the fragmentation approximation is that it does not retain information about the associated jets from the $\bar{b}$ and $\bar{c}$ meson, which are very important in experiments. At LHC the dominant production of the B_c meson will be gluon-gluon fusion, $gg \rightarrow B_c + c + \bar{b}$. The Feynman-diagram of the gg-fusion can be seen in Fig. 1.12.

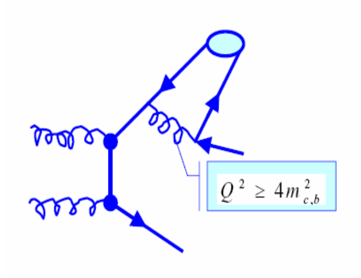

Fig. 1.12 Feynman diagram of gluon gluon fusion

This process is of the fourth order of the strong coupling constant and there exist 36 such Feynman diagrams. The calculation of the total square amplitude, which is the sum of all the diagrams squared, is difficult due to the large number of terms. Another thing that makes these amplitude calculations unpractical is that a Monte Carlo simulation based on these calculations would be very time consuming. Using the helicity technique solved these problems. This technique gave reliable results and from these calculations a Monte Carlo generator for gluon-gluon fusion called BCVEGPY [22], was created.

1.6 Event simulations

In order to investigate what to expect and look for in experiments event simulations are used. Different simulation programs are needed for the different steps in the simulation. A summary of the programs can be found in Table 1.4 and a schematic view of the parts involved in the generation of an event can be seen in Fig 1.13.

	Assignment	**Used**
Event generator	Produces the particles created in a collision between two accelerated particles.	PythiaB
Particle generator	Some particles are not defined in Pythia and these have to be created in a separate generator.	BCVEGPY2.0 (Produce B_c mesons)
Decay generator	Decays the particles in the event. Handles for example momentum and decays of the created particles.	EVTGEN
Detector simulator	Simulates the functioning of the detectors and gives out "detection signals".	Athena + Geant4
Event analyzer	Analyzes the signal from the detector simulation by using an algorithm written by the user.	
	Ties together all the ends from the different steps and makes a complete chain.	Athena

Table 1.4 Brief description of the simulation programs.

The standard event generator is Pythia [23] and **PythiaB** is an ATLAS modification for $b\bar{b}$ -events. The events are generated with the use of Monte Carlo technique. The theory of how physical events occur is not known exactly and therefore variables are set by probability distributions, such as parton distributions. Parton distributions are called parton density functions and they are functions telling how probable it is to find a specific quark inside a proton.

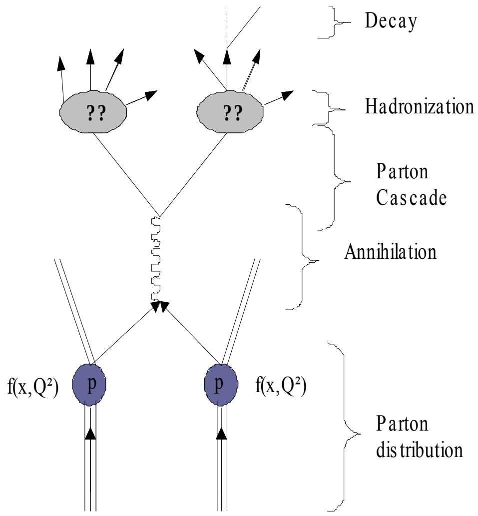

Fig. 1.13 Schematic view of the parts involved in generating an event [24].

The hadronization process is one of the questions that physicists still have no definite answer to. There are several models that predict how it occurs, one of them is the Lund string model and this is the one that is used in PythiaB. B-quark production is suppressed about 1/100 at LHC energy. To speed up the simulation PythiaB uses the same b-quark in several hadronizations. This leads to larger statistics in a shorter time and since it is a random process large statistics is important to come as close as possible to the reality.

BCVEGPY2.0 generates S and P states of the B_c meson. In the calculations only the gluon gluon fusion mechanism is taken into account for the P states. For the S states the light quark-antiquark annihilation process in taken into as well, calculations in Ref. [25] show that the contribution of light quark-antiquark annihilation is of the order ~1%.

EVTGEN makes the beauty hadrons generated by PythiaB decay.

Athena uses a defined algorithm to analyze the events that are given to it. All this is set in the jobOption file.

Fig. 1.14 gives a summary and an overview of the software packages needed for the full simulation of the B_c mesons. Since in this work the $B^+(J/\psi\ K^+)$ mesons were used instead of the B_c mesons for optimizing the analysis (see 2.2.1 and 3.1), there was no need for using BCVEGPY2.0 nor EVTGEN. The program flow for the B^+ case is marked with the dash-dotted line in Fig. 1.14.

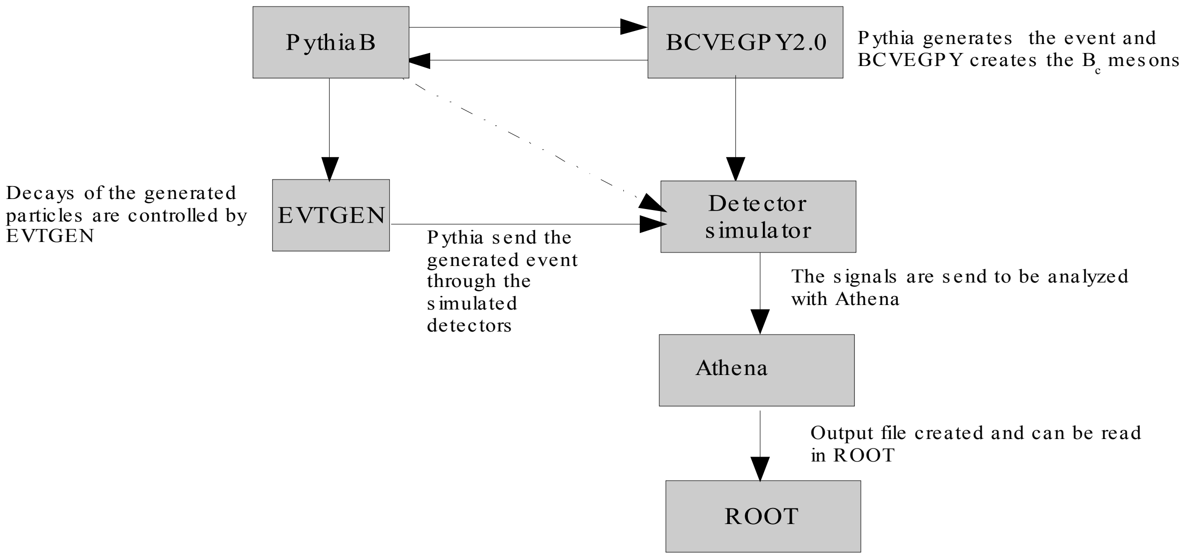

Fig. 1.14 Diagram of the software path for simulating B_c events. The program flow for simulating the corresponding B^+ sample is marked with the dash-dotted line.

In a simulation the right answer is always available since it is we that have created the events and thus we know the content of them. This property enables us to check how good our analysis code is and it also gives the possibility to make estimations on numbers such as the muon identification efficiency. As a summary, simulations can be seen as a test environment where optimization of the analysis code is possible.

2 The Process

To get a better understanding of the strong force we are interested in finding a way to detect different mass states of B_c. In this section the B_c signal and backgrounds are discussed. Some of the questions of importance for the simulations are answered in this section. For example which decays are detectable? How should they be reconstructed? and How many of them should we expect to find?

2.1 The B_c signal

When searching for interesting events in a data sample one goes backwards step-by-step and in each step the number of candidates is reduced by requirements set by the user. In our search the first step is to find events where there is a decay of the ground state B_c meson. The identity signal of the ground-state decay is:

- Two muons with an invariant mass compatible with the mass of J/ψ.
- One positive pion that goes through the same vertex as the muons, and which together with the muons has an invariant mass compatible with the mass of B_c.

This analysis considers only B_c^+ with π^+ in the final state but in the real analysis the charge conjugated states are included as well .The corresponding antiparticle will thus be reconstructed in a similar way by requiring a negative pion insted of the positive one.

The decays of B_c* which are easiest to study in ATLAS are the ones decaying into hadrons. The hadronic final state has two pions and gives a clear signal while the radiative decays involve a low-energy photon which is impossible to detect in ATLAS. The hadronic decays can be seen in Fig 2.1.

Decay 1:

$$B_c(2^1S_0) \to B_c(1^1S_0) + \pi^+ + \pi^-$$

$$\hookrightarrow J/\psi + \pi \to \mu^+ + \mu^- + \pi$$

Decay 2:

$$B_c(2^1S_1) \to B_c(1^1S_1) + \pi^+ + \pi^-$$

$$\hookrightarrow B_c(1^1S_0) + \gamma$$

$$\hookrightarrow J/\psi + \pi \to \mu^+ + \mu^- + \pi$$

Fig 2.1 The hadronic decays of B_c.

When looking for the excited decays two soft pions are added to the B_c signal. Due to the short lifetime of the excited state and J/ψ all the particles produced in the decay chain will be seen as coming from the same vertex, see Figs 2.2 and 2.3.

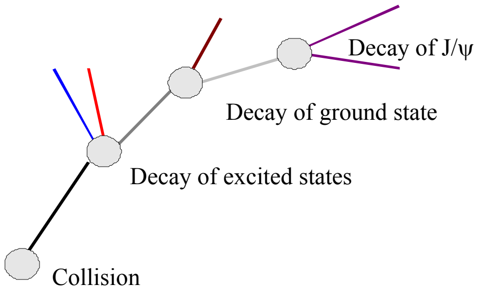

Fig 2.2 Schematic view of the decay.

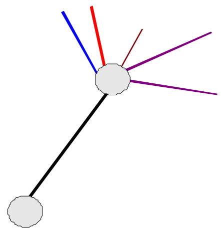

Fig 2.3 Detected ("seen") signal.

2.2 Optimization

To get a significant B_c signal from an experiment the cuts in the analysis code have to be chosen so that as many as possible correct events are selected, while the background events are rejected. This procedure is the optimization and is done with help of simulated data.

2.2.1 The signal

The $\bar{b}c$ system is a fairly unknown system. For example, there are large theoretical uncertainties in the production mechanism in pp-collisions. This introduces uncertainties to the B_c simulations and consequently the optimization will not be accurate. Therefore a better-known system with similar kinematics is used. The $\bar{b}u$-meson B^+(J/ ψ K^+) fulfills the requirements of being theoretically well known and similar to B_c(J/ ψ π^+). The two mesons differ significantly both in mass and lifetime but their decay channels look the same except for that the positive pion in the B_c decay is a positive kaon in the B^+ decay. This is exactly what the CDF experiment at Fermilab did when analyzing the B_c(J/ ψ π^+) -decays[26].

2.2.2 The background

In the optimization it is necessary to consider background effects in the J/ ψ reconstruction and in the B_c reconstruction.

When reconstructing J/ ψ the critical step is when muon pairs are combined. Since false muon combinations i.e. false J/ψ will have a more or less flat mass distribution, they will not give a large effect. Combining a true J/ ψ with a third particle not originating from the same B_c decay produces false B_c mesons. This third particle can come from the primary vertex or other B decays. The fake combinations in which the third particle comes from another B decay in the same event will not have a flat mass distribution. The fake mass will lie somewhere near the B_c mass and consequently giving false contributions to the B_c reconstruction. Thus we can conclude that in the optimization of the analysis code we have to check the cuts against a background corresponding to B→ J/ψX, where X is any particle or several particles, and "B" is any B-hadron.

2.3 Number of events

The number of observed B_c^* events N_{events} is given by Eq. 2.1:

$$N_{events} = L\, t\sigma(pp \to \bar{b}b|_{|\eta|<2.5,\, p_T(\mu)>6}) \times P(b \to B^*_c) \times BR(B^*_c \to B_c\pi^+\pi^-) \times BR(B_c \to J/\psi\pi) BR(J/\psi \to \mu^+\mu^-) \cdot \varepsilon_{trig} \cdot \varepsilon_{analys} \qquad (2.1)$$

The number of observed ground state events B_c is given by Eq. 2.2:

$$N_{events} = L\, t\sigma(pp \to \bar{b}b|_{|\eta|<2.5,\, p_T(\mu)>6}) \times P(b \to B_c) \times BR(B_c \to J/\psi\pi) \times BR(J/\psi \to \mu^+\mu^-) \cdot \varepsilon_{trig} \cdot \varepsilon_{analys} \qquad (2.2)$$

All the elements and their estimated value are given in Table 2.1. The Table includes assumptions (luminosity, time), values from literature (probability, branching fractions and cross-section), and efficiencies obtained in this study (see chapter 3.3.1).

Element		***Description***	***Estimation***	***[ref]***
L		Luminosity	$2\times 10^{33} cm^{-2} s^{-1}$	[27]
t		The time samples are collected.	1 effective year = 10^7s	
$\sigma(pp \rightarrow \bar{b}b \rightarrow \mu X \|_{\|\eta_\mu\|<2.5 \quad p_T(\mu)>6GeV})$		The cross-section for a pp collision to create a beauty pair with at least one muon in the final sate and with restrictions on pseudorapidity and transverse momentum on the muon.	3.63 μb	[28]
$P(b \rightarrow B^*_c)$		Probability for b-quark to hadronize into a B_c^* meson	3.6×10^{-4}	[21]
$P(b \rightarrow B_c)$		Probability for b-quark to hadronize into a B_c meson	1.5×10^{-3}	[21]
$BR(B_c \rightarrow B_c\pi^+\pi^-)$	$B_c = 2^1 S_0$	Branching ratio for an excited B_c meson to decay to the ground state via emitting two pions	74 %	[18]
	$B_c = 2^1 S_1$		58 %	[18]
$BR(B_c \rightarrow J/\psi\pi)$		Branching ratio for the B_c meson to decay to charmonium and a pion	0.2 %	[29]
$BR(J/\psi \rightarrow \mu^+\mu^-)$		Branching ratio for charmonium to decay to two muons	5.93±0.06 %	[3]
ε_{trigg}		The dimuon trigger efficiency	61.0 ±0.4 %	[30]
ε_{analys}		The efficiency of this analysis. The efficiency includes many components. One estmated axample is example is the combined muon id efficiency	64.3 % 97.4 %	

Table 2.1 Elements to needed to get an estimation on the number of events.

2.4 Estimations

2.4.1 Dimuon trigger efficiency

The trigger described in 1.3.4 is a single muon trigger, but the upgraded version of the trigger and the trigger that is used here is the dimuon trigger. In the dimuon trigger there are regions where the trigger chambers geometrically overlap. In these regions it is possible that one muon incorrectly triggers a dimuon event, these are called false dimuons. To prevent this flags are set in the trigger logic, there is one η flag and one φ flag. The η– and φ - coordinates give the muon's position and the associated flags are set in such a way that if the coordinates of two muons could come from one muon the event is ignored.

The dimuon trigger efficiency has been studied in ref. [30]. The trigger efficiency is given by:

$$\varepsilon_{trigg} = \frac{number\ \ of\ \ events\ \ passing\ \ the\ \ trigger}{number\ \ of\ \ actual\ \ events} \tag{2.3}$$

There were three scenarios investigated; (1) the efficiency without any flags, (2) with only η flag and (3) with both flags. The results obtained for multiple muon events are presented in Table 2.2.

Flags used	Trigger efficiency
Without flags	(58.4 ±0.3)%
With η flag	(59.0 ±0.4)%
With both overlap flags	(61.0 ±0.4)%

Table 2.2 Table of trigger efficiencies for muon events with at least two muons.

We can note that the dimuon trigger efficiency is relatively low but this is the efficiency for two muons. The single muon trigger has approximately the efficiency $\sqrt{0.61} = 0.781$. The 21.9 % loss in trigger efficiency is due to that the muon trigger does not cover the whole detector, there are for example no trigger chambers in the areas where the legs of the detector are located.

2.4.2 Combined muon identification efficiency

The muon identification efficiency is given by:

$$\varepsilon_{\mu id} = \frac{number\ \text{of}\ \text{det}ected\ muon\ pairs}{number\ of\ generated\ muon\ pairs} \tag{2.4}$$

The detected muons are taken as the track pairs that form the J/ψ-candidates. The selection of the J/ψ-candidates will be described in section 3.2. The generated muons are the actual number of muons generated. In this case this number is equivalent to the number of B^+ decays since only the signal events are used.

3. Analysis of the B^+ signals and backgrounds

3.1 Event samples

As the signal a sample consisting of 20 000 $B^+ \rightarrow (J/\psi(\mu^-\mu^+)\ K^+)$ events was used. These events were generated by using PythiaB and passed through the full ATLAS simulation by Christos Anastopoulos at Thessaloniki University. As a background a sample of 40 000 $b\bar{b} \rightarrow (J/\psi\ X)$ was used, where X is any particle or several which can occur in allowed B-hadron decays in addition to the J/ψ.

3.2 Reconstruction of the B^+ signal

The decay of B^+ gives a secondary vertex from which two oppositely charged muons and one positive pion comes from. In the reconstruction of this signal the muons are first picked out by applying p_T and η cuts ($p_T(\mu)$>6 GeV and $|\eta(\mu)|$<2.5). Pairs are created and the ones that have oppositely charged muons are picked out and passed through transverse momentum and η cuts. The invariant mass of the pairs passing those cuts are calculated and compared to the J/ψ mass. The pairs with an invariant mass more than 150 MeV from the nominal J/ψ mass are discarded, the ones remaining will be fit into a vertex. The following vertex cuts are applied: good vertexing, χ^2 and fit-mass cuts. The good vertexing is a logical function that is a class member of the class Vertex in the analysis code (written in C++). The function tells if the secondary vertex fitting is converging. If some errors occur, or if it is unlikely that the tracks originate from the same vertex this function returns false, otherwise it returns true.The χ^2 cut lets candidates with χ^2/NoF below a set value to pass. The fit-mass cut compares the reconstructed mass at the vertex with the known J/ ψ mass as given in the Particle Data Book [3] and lets the ones that are within 100 MeV from the J/ ψ mass to pass. The pairs now remaining are the J/ ψ -candidates. A summary of the cuts is given in Fig 3.1 and an example of how the mass distribution of the reconstructed pairs looks like is shown in Fig 3.2.

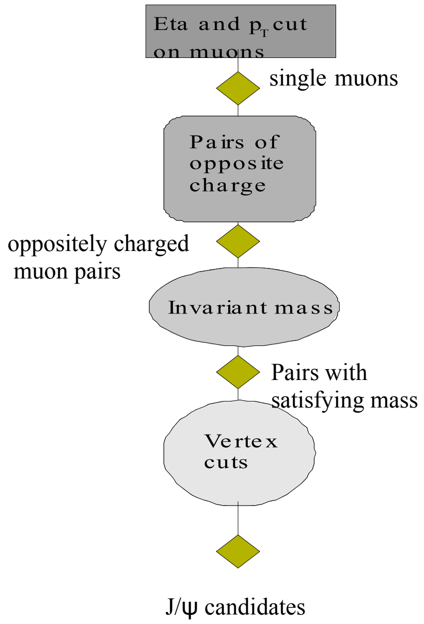

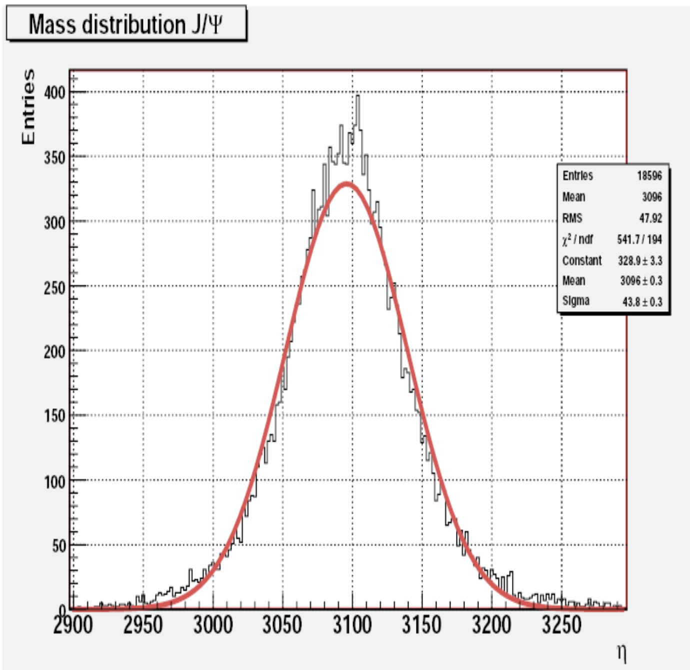

Fig 3.1 Schematic view of the J/ψ selection. Fig 3.2 The reconstructed J/ψ mass in signal events.

The kaon candidates are selected by applying transverse momentum and η cuts on all tracks (p_T> 1.5GeV and |η|<2.5). The particles previously identified as muons are removed and only particles with a positive charge are considered.

To get the B^+ candidates all possible triplets are formed from the J/ψ - and kaon candidates, the invariant mass of the triplets is calculated and passed through a loose mass cut of ± 600 MeV. Then vertexing is done: good vertexing, χ^2 and fit-mass cuts are applied. Finally all the candidates are passed through a decay length cut, and the ones passing are the B^+ candidates. A summary of the cuts for B^+ is given in Fig 3.3 and an example of how a mass distribution from signal events looks like is seen in Fig 3.4.

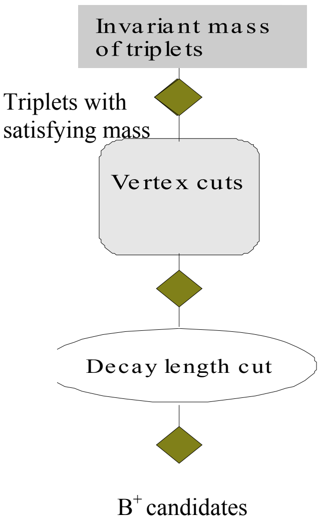

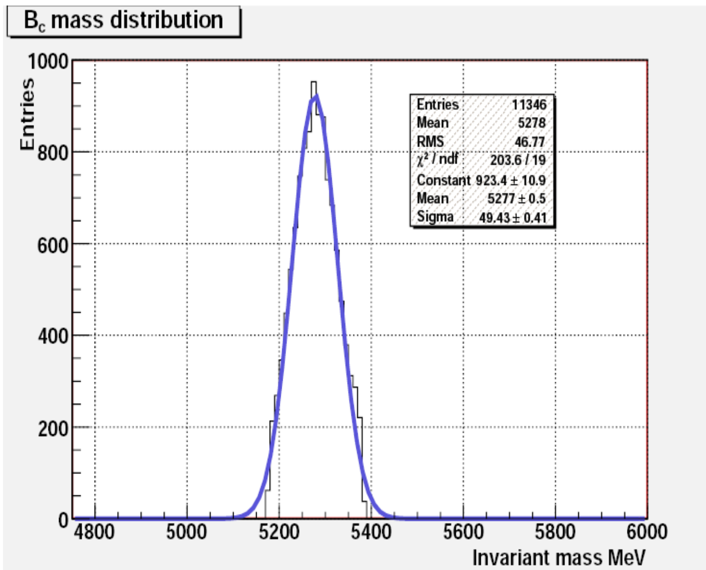

Fig 3.3 Schematic view of the B^+ selection. Fig 3.4 The reconstructed B^+ mass in signal events.

The values of the cuts used in the analysis are shown in Table 3.1.

Cut	$\mu^+ \mu^-$	***Kaon***	B^+
p_T	>6 GeV	>1.5 GeV	----
$\|\eta\|$	< 2.5	< 2.5	----
|inv.mass-PDGmass|	< 150 MeV	----	< 500 MeV
χ^2**/Nof**	< 5	----	< 10
|fit-mass-PDGmass|	< 100 MeV	----	<3σ
Decay length	----	----	>430 μm

Table 3.1 Table of cuts for J/ψ, Kaon and B^+. PDGmass = mass according to Particle Data Group, σ=60 MeV.

The transverse momentum cut for the muons is set to 6 GeV since it is this value that is used at LVL1 trigger when events for further investigation are chosen. The transverse momentum cut for the kaons is set to 1.5 GeV because this reduces the background from particles created in the primary vertex.

The fiducial coverage of the inner detector is the reason for the η cut both for muons and kaons. The invariant mass cuts are set to a value that will keep most of the interesting events and limit the background. The χ^2 cut is set to a value of the order of ten so that bad fits are discarded, while it is big enough so that we don't loose signal events. The fit-mass cut is set to three standard deviations, because this assures that the majority of signal events will pass. The decay length of the B_c meson is set to a minimum of $2\sigma_d$, σ_d is the primary vertex resolution, to be certain that it has a displaced secondary vertex. The simulated particle is the B^+ instead of the B_c meson and thus the decay length cut is scaled according to their lifetimes, Eq 3.1:

$$decayLength(B^+) = decayLength(B_c) \cdot \frac{\tau(B^+)}{\tau(B_c)} \qquad (3.1)$$

where decayLength(B_c)= $2\sigma_d$ =2*60 μm [31], $\tau(B_c)$ = 0.46 ps and $\tau(B^+)$=1.64 ps [3]. For the background the decay length cut used was decayLength > $2\sigma_d$, i.e. the same as for the real B_c signal.

3.3 Results

When generating the background events the cross-section was 4 nb [28]. In this cross-section the following parts are included in, Eq. 3.2:
- $p_T(\mu)$>6 GeV
- $|\eta|<2.5$
- BR(b→J/ψ X) = 0.05101
- BR(J/ψ → $\mu^+\mu^-$) = 0.06
- Symmetry correction 2

$$\sigma_{backg} = 2\times\sigma(pp\to \bar{b}b|_{|\eta|<2.5,p_T(\mu)>6GeV})\times BR(b\to J/\psi X)\times BR(J/\psi\to\mu^+\mu^-) = 4\ \ nb \qquad (3.2)$$

In the signal generation only the momentum requirement for a muon and the η restriction are included in the cross-section and the value is 3.64 μb, Eq. 3.3.

$$\sigma_{b\to\mu X} = \sigma(pp\to \bar{b}b|_{|\eta|<2.5,p_T(\mu)>6GeV}) = 3.64\ \ \mu b \qquad (3.3)$$

To get the true cross-section for the signal the symmetry correction and branching ratios have to be included. The B^+ meson is used only to get reliable simulations and the meson that is of interest is the B_c meson, thus the numbers in Table 2.1 are used to get a cross-section for the B_c meson (Eq. 3.4):

$$\sigma_{signal} = \sigma_{b\to\mu X}\times 2\times P(b\to B_c)\times BR(B_c\to J/\psi\pi)\times BR(J/\psi\to\mu^+\mu^-) =$$
$$3.64\mu b\times 3.6\cdot 10^{-7} = 1.31\ \ pb \qquad (3.4)$$

3.3.1 Efficiencies

The muon identification efficiency obtained from the analysis is:

$$\varepsilon_{\mu id} = \frac{number\ \ of\ \ detected\ \ muon\ \ pairs}{number\ \ of\ \ generated\ \ muon\ \ pairs} = \frac{19476}{20000} = (97.4\pm 1.4)\% \qquad (3.5)$$

The efficiency of the whole analysis, which incorporates the combined muon identification and the analysis are given for the signal events in Eq.
(3.6) and for the background events in Eq. (3.7). The background events are selected in the region $|m-m(B_c)|\leq 3\sigma$.

$$\varepsilon_{signal} = \frac{number\ \ of\ \ events\ \ passing}{number\ \ of\ \ events\ \ inserted} = \frac{12852}{20000} = (64.3\pm 1.0)\% \qquad (3.6)$$

$$\varepsilon_{backg} = \frac{number\ \ of\ \ events\ \ passing}{number\ \ of\ \ events\ \ inserted} = \frac{257}{40000} = (0.64\pm 0.04)\% \qquad (3.7)$$

3.3.2 Reconstruction

The mass distributions of J/Ψ and B_c obtained in the analysis can be seen in Figs. 3.5 and 3.6 along with statistics of the fits in Tables 3.3 and 3.4.

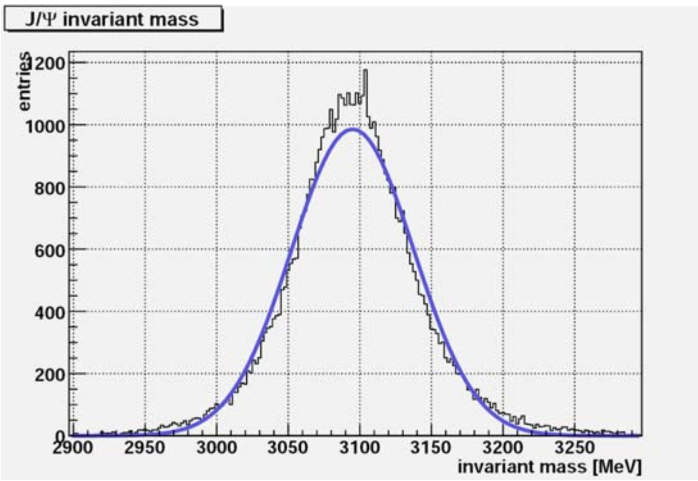

Entries	**54295**
Mean	**3096 MeV**
RMS	**46.95 MeV**
Chi²/NoF	**8.17**
Sigma	**42.64 MeV**

Fig 3.5 Mass distribution of J/ Ψ.

Table 3.3 Statistics of fit to J/ Ψ distribution.

The measured J/ψ mass is thus (3.096 ± 0.043) GeV. This is consistant with previous ATLAS studies, and there is no bias on the J/ψ mass (world-avarage measurement for the J/ψ mass is 3096.916 MeV)

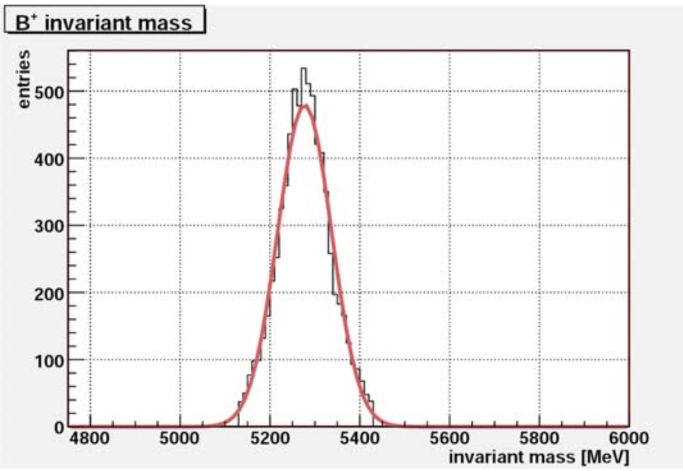

Entries	**7207**
Mean	**5278 MeV**
RMS	**58 MeV**
Chi²/NoF	**3.08**
Sigma	**(60.05±0.70) MeV**

Fig 3.6 Mass distribution of B^+.

Table 3.4 Statistics of fit to B^+ distribution.

The measured B^+ mass is thus (5.278 ± 0.060) GeV. This is also consistant with the expected mass resolution in ATLAS.

3.3.3 Number of events

When plugging in assumptions, known values, and the estimated values obtained in this study into equation 2.1 we get that the number of expected number of produced B_c and B_c^* events at LHC will be 26208 and respectively 9435. In Table 3.5 it can be seen how the number of B_c signal and background events decreases step-by-step. The final number of signal B_c-events is 10 272 for 20 fb^{-1}.

	LHC	**Trigger (61 %)**	**Analysis**
Signal			
$P(b \rightarrow B_c)$	218 400 000		
$BR(B_c \rightarrow J/\psi\pi)$	436 800		
$BR(J/\psi \rightarrow \mu^+\mu^-)$	26 208	15 986	10 272
Background			
	80 000 000	48 800 000	313 320

Table 3.5 Estimated numbers of B_c and background events produced, passing the trigger and passing the analysis at LHC. The assumed integrated luminosity is 20fb^{-1} (1 year at $L= 2 \cdot 10^{33} cm^{-2}s^{-1}$)

3.3.4 Normalized results

The ratio between the signal and background used in the simulation does not reflect the reality. In Table 3.6 the number of events produced at LHC in one year, the number of events used in the simulation and the number of events that passed the simulation are given. As can be seen the number of simulated background events is far below the real statistics. The background statistics is limited by available computing resources.

	LHC	**Simulation**	**Analysis**
Signal	26 208	20 000	12 852
Background	80 000 000	40 000	257

Table 3.6 Number of signal and background events produced at LHC, used in the simulation and passed the analysis

The normalized mass distribution diagram for the background can be seen in Fig 3.7 after all the other cuts apart from the final mass cut. Notable is the peak at ~5200 MeV, these entries are true B^+ mesons found in the backgound.

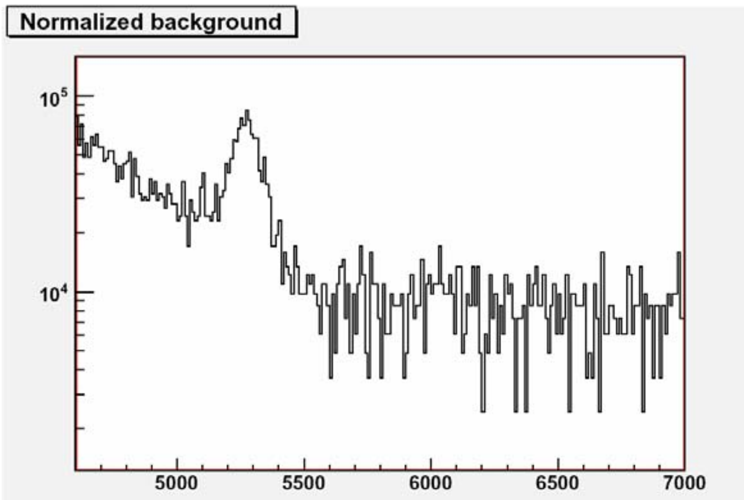

Fig. 3.7 Normalized mass distribution of the background.

The mass distribution for the B^+ signal normalized according to B_c branching ratios is seen in Fig. 3.8. The x-axis is shifted so that the mass is centered at the B_c mass.

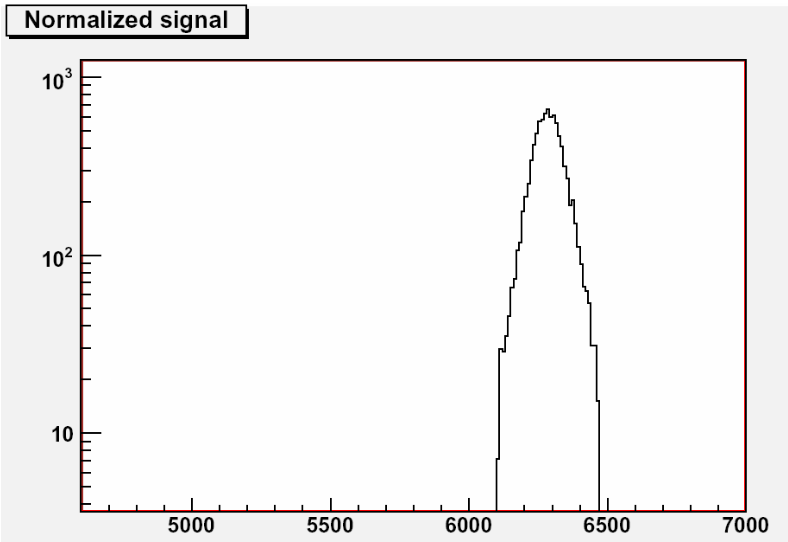

Fig. 3.8 Normalized mass distribution for the B^+ (B_c) signal.

In the mass distribution for the signal and background together, Fig. 3.9, the signal peak is not visible. This is due to that the background statistics is not representative for the real background and consequently the bin-to-bin fluctuations are bigger than they will be in reality.

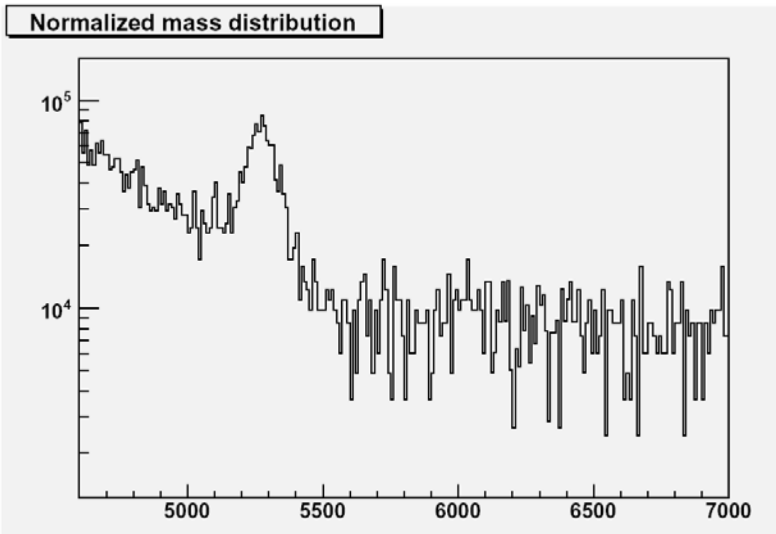

Fig. 3.9 Normalized mass distribution for the signal+background.

For a signal to be observable the significance of the signal should be at least five standard deviations above the background, Eq. 3.8:

$$\frac{signal}{\sqrt{background}} > 5 \qquad (3.8)$$

In this analysis the normalized background is 313 320 events within the 3σ mass region (± 180 MeV) around the B_c mass, and the signal is 10 272 inside the same mass regions. These numbers gives a value of 18.4 and thus it can be concluded that the B_c signal is detectable. The significance could be further improved by narrowing down the accepted mass region. Table 3.7 gives a summary of the signal significance when different mass cuts are used.

Mass cut	**Signal**	**Background**	**Signal signicance**
$m(B_c) \pm 3\ \sigma$ (± 180 MeV)	10 272	312 320	18.4
$m(B_c) \pm 2\ \sigma$ (± 120 MeV)	8 599	202 520	19.1
$m(B_c) \pm 1\ \sigma$ (± 60 MeV)	6 633	130 700	20.6

Table 3.7 The signal significance at three different mass cuts.

3.4 Discussion and conclusion

It can be concluded that it is possible to reconstruct the decays $B^+ \rightarrow J/\psi K^+$, $J/\psi \rightarrow \mu^+\mu^-$ and thus it should be possible to do the same for B_c mesons when B_c decays into $J/\psi\pi^+$, and $J/\psi \rightarrow \mu^+\mu^-$. These decays have similar kinematics. They differ by that there is a pion in the B_c decay instead of the kaon that is involved in the decay of B^+. There are also other differences between the two mesons which lead to necessary changes in the analysis for B_c. For instance, the mass is higher for the B_c meson, and it has a shorter lifetime. The decreased lifetime may have larger effects than just changes in the cuts. Because the distance between the primary and the secondary vertex will be on the average smaller for the B_c meson (~490 μm for B^+ and ~140 μm for B_c) the decay length cut has to be reoptimized and the analysis is approaching the limit given by the decay length resolution (σ=60 μm). Clearly a simulated sample of B_c-mesons would be needed to study this effect.

The next step in the B_c studies would be to investigate the possibility to detect excited states 2^1S_0 and 2^1S_1. As it is stated in section 2.1 the hadronic decays are the ones of interest, and as can be seen in Fig 2.1 these two decays differ by a photon. This photon will have the approximate energy of 70 keV and consequently it is not possible to detect it in the detector. Looking for a photon cannot therefore separate these decays, instead they will have exactly the same detectable particles going out from the decay vertex. This in turn will lead to that the peak B_c mass will be a sum of the two mass states, when in reality they are separated by 70 keV. There is a need for something else to be able to separate the two mass states. One possible solution can be using the angular distributions, because decay 1 ($2^1S_0 \rightarrow 1^1S_0$) in Fig 2.1 is a decay of a pseudoscalar ($J^p=0^-$) state to another pseudoscalar state while the decay 2 ($2^1S_1 \rightarrow 1^1S_1$) is a decay from a vector state ($J^p=1^-$) to another vector state. The angular distributions of the two decays are thus not identical and we have something that distinguishes the decays and this could be a way to separate the two mass states.

Acknowledgment

A big thank you to Birgitte Epp for helping me with getting started with the software and I also would like to thank her, Partick Jussel and everyone else at Leopold-Franzens-University who made my visit pleasant. Thank you also to Christos Anastopolos and Maria Smizanska who have helped me with files, file storage and all questions involving files. Of course I would like to thank my supervisor Paula Eerola for good guidance. And last of all I would like to thank Thomas Nilsson for being patient and listened to me though you haven't had a clue what I have talked about!
Without all of you this would not have been possible.

References

1. http://nobelprize.org/nobel_prizes/physics/laureates/2004/public.html
2. B.R Martin and G. Shaw, "*Particle Physics*", ISBN 0-471-97252-5
3. Particle Data Group, http://pdg.lbl.gov
4. "*Pseudo-Rapidity, Azimuthal Angle, and Transverse Momentum*", http://www.phys.ufl.edu/~rfield/cdf/chgjet/etaphi.html
5. ATLAS collaboration, "*Atlas detector and physics performance, Technical Design Report Volume 1*", CERN/LHCC/99-14, (May 1999)
6. S. George, "*ATLAS: Triggers for B-physics*", ATL-COM-CONF-99-011, Nucl. Ins. And Meth. A 446 274-281 (2000)
7. René Brun *et al*., "*ROOT: Users Guide 5.14*", ftp://root.cern.ch/root/doc/Users_Guide_5_14_TwoInOne.pdf
8. F. Abe *et al.* ,"*Observation of B_c mesons in pp-collisions at sqrt[s]=1.8 TeV*", Phys. Rev. D58 112004 (1998)
9. A. Kumar Rai and P.C. Vinodkumar, "*Properties of the B_c meson*", Pramana –J.Phys. Vol. 66 No. 5 (May 2006)
10. A. Abd El-Hady, M.A.K. Lohdhi and J.P. Vary, "*B_c mesons in Bethe-Salpeter model*",Phys. Rev. D59, 094001 (1999)
11. Barate R. *et al* ., "*Search for the B_c meson in hadronic Z decays*", Phys. Lett. B402, 213 (1998)
12. P. Abreu *et al., "Search for the B_c Meson",* Phys.Lett B398, 207 (1997)
13. K. Ackersta *et al*., *"Search for the B_c Meson in Hadronic Z0 Decays"* , Phys. Lett. B420, 157 (1998)
14. A. Abulencia *et al.* ,*"Evidence for the exclusive decay $B_c^+ \rightarrow J/\psi\ \pi^+$ and measurement of the mass of the B_c meson",* Phys. Rev. Lett. 96 (2006) 082002
15. A. Abulencia *et al.* ,*"Measurement of the B_c Meson Lifetime Using $B_c \rightarrow J/\psi\ e\nu$",* Phys. Rev. Lett. 97 (2006) 012002
16. W. Buchmüller and S. -H. H. Tye,"Quarkonia and quantum chromodynamics", Phys. Rev. D24, 132 (1981)
17. A. Martin, "*A fit of Upsilon and Charmonium spectra*", Phys. Lett. B93, 338 (1980)
18. I.P Gouz, V.V. Kiselev, A.K. Likhoded,V.I. Romanovsky and O.P. Yushchenko, "*Prospects for the B_c Studies at LHCb*", asXiv:hep-ph/0211432 v1, 27Nov2002
19. K. Cheung ,"*B_c meson production at hadron colliders by heavy quark fragmentation*", Phys. Rev. Lett 71, 3413 (1993)
20. A. Leike and R. Rückl, "*Production of the heavy bound states at LEP and beyond*", Nucl. Phys. B Proceedings Supplements 37, 215 (1994)
21. E. Braaten, K. Cheung and T.C. Yuan ,"*QCD fragmentation functions for B_c and B_c^** production", Phys. Rev. D48, 5049 (1993)
22. C. Driouichi, "*B-physics potential of the ATLAS experiment and performance of the ATLAS Transition Radiation Tracker*", Doctoral Thesis by Chafik Driouichi (2004)
23. Torbjörn Sjöstrand, Stephen Mrenna ans Peter Skands, "*PYTHIA 6.4 Physics and Manual*", hep-ph/0603175
24. "*Detector simulations, exclusive search and mass measurements for Supersymmetry at ATLAS*", diploma thesis by Marianne Johansen at Oslo University.
25. C.H. Chang, J.X. Wang and X.G. Wu, *"BCVEGPY2.0: A upgraded version of the generator BCVEGPY with an addendum about hadroproduction of the P-wave B_c states",* arXiv:hep-ph/0504017 (2005)

26. CDF collaboration, "*B_c^- → J/ψ π⁻ at CDF with 1.1 fb^{-1}*", CDF note 8004, http://www-cdf.fnal.gov
27. P.J. Bell, "*The precision reach of ATLAS for electroweak physics in the low luminosity era*", arXiv:hep-ex/0405015 (2004)
28. E.V. Bouhova-Thacker, " *"Model" for bb → J/ ψX Generation*", http://msmizans.home.cern.ch/msmizans/production/dc2/generators/Btojpsix_note.pdf
29. M. Lusignoli and M. Masetti, "*B_c decays*", Z. Phys. C 51, 549(1991)
30. T. Lagouri, N. Kanaya and A. Krasznahorkay, "*B-physics and LVL1 dimuon trigger in the ATLAS experiment at the LHC",* ATL-COM- PHYS-2006-007
31. N. Benekos *et al. ,"B-physics performance with Initial and Complete Inner detector layout in Data Challange 1",* ATL-PHYS-1005-002